Communication

# Size-Controlled Assembly of Gold Nanoparticles Induced by a Tridentate Thioether Ligand

Mathew M. Maye, Jin Luo, I-Im S. Lim, Li Han, Nancy N. Kariuki, Daniel Rabinovich, Liu, and Chuan-Jian Zhong

*J. Am. Chem. Soc.*, **2003**, 125 (33), 9906-9907• DOI: 10.1021/ja0363866 • Publication Date (Web): 23 July 2003



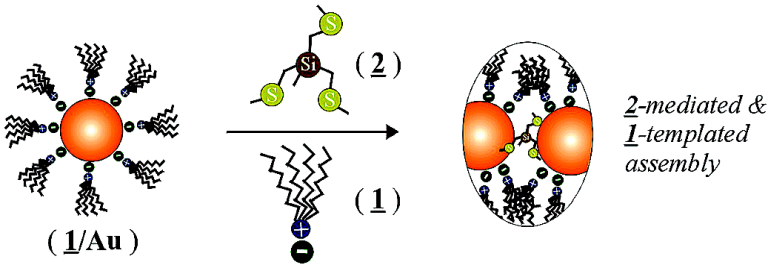


## More About This Article

Additional resources and features associated with this article are available within the HTML version:

- Supporting Information
- Links to the 13 articles that cite this article, as of the time of this article download
- Access to high resolution figures
- Links to articles and content related to this article
- Copyright permission to reproduce figures and/or text from this article

View the Full Text HTML

J|A|C|S
COMMUNICATIONS

Published on Web 07/23/2003

# Size-Controlled Assembly of Gold Nanoparticles Induced by a Tridentate Thioether Ligand

Mathew M. Maye,[†] Jin Luo,[†] I-Im S. Lim,[†] Li Han,[†] Nancy N. Kariuki,[†] Daniel Rabinovich,[‡] Tianbo Liu,[§] and Chuan-Jian Zhong*,[†]

*Department of Chemistry, State University of New York at Binghamton, Binghamton, New York 13902, Department of Chemistry, The University of North Carolina at Charlotte, Charlotte, North Carolina 28223, and Department of Physics, Brookhaven National Laboratory, Upton, New York 11973*

Received May 28, 2003; E-mail: cjzhong@binghamton.edu

The ability to assemble nanoparticles with controllable sizes and shapes is increasingly important because many frontier areas of research such as sensors, catalysis, medical diagnostics, information storage, and quantum computation require the precise control of array architecture and component miniaturization. Most existing approaches explore the strong affinity of thiols to gold or silver (e.g., monolayer-capping via two-phase synthesis,[1] place-exchanging,[2] stepwise assembling,[3−6] DNA linking,[7−9] or hydrogen-bonding[10,11]) and the use of disulfides[12] and thioethers[13] as capping agents as well. Polymers functionalized with molecular recognition groups,[14] thioacetate groups,[15] and tetradentate thioether ligands[16] have recently been used to mediate the formation of spherical or related assemblies of gold nanoparticles. While these approaches have shown remarkable capabilities in assembling nanoparticles into functional nanostructures, the ability to control their size and shape has not been fully realized. Here, we report a novel mediator-template route that explores the molecular driving forces exerted by the tridentate thioether $MeSi(CH_2SMe)_3$ (**2**)[17] as a mediator and tetraoctylammonium bromide $[CH_3(CH_2)_7]_4N^+Br^-$ (**1**) as a templating agent toward the unprecedented size-controlled formation of spherical assemblies of gold nanoparticles. A simple combination of molecular driving forces is exploited in this mediator-template strategy, which is demonstrated for the **2**-mediated assembly of **1**-capped gold nanoparticles (abbreviated as **1**/**Au**). There are two important forces controlling this process. The first is the mediation force as a result of the coordination ability of **2** to Au, which can be manipulated by the number of thioether groups on **2**. We have recently demonstrated this viability for forming spherical assemblies of ∼60 nm diameter with a tetrathioether.[16] The second is the templating effect exerted by the surfactant reactivity of **1**. Surfactant-based micellar templating effects are well-documented for aqueous solutions,[18] where the shape formation (spheres, rods, etc.) depends on the structure and the concentration of surfactants. Theory[18] predicts that spheres usually prevail when the relative geometric ratio of surfactant versus packing structure is below a critical value.

Gold nanoparticles capped with tetraoctylammonium bromide and the tridentate ligand **2** were used to demonstrate the formation of spherical assemblies via the mediator-template route. **1**/**Au** particles with an average core size of 5.1 (±0.9) nm were synthesized according to Schiffrin's protocol[19] and were stored in the reaction solution (toluene) containing **1** (∼25 mM). As shown in Figure 1, the combination of **1** and **2** led to the formation of spherical assemblies of Au nanoparticles of relatively high monodispersity. The size of the spherical assemblies is dependent on the relative ratio of **2** versus **1**/**Au** ($r$). The crystallinity of the individual nanocrystals is shown by the HRTEM (insert); the close-packed ordering of the assembled nanocrystals can be resolved along the edges of the spheres (Figure 1b). Spheres of different sizes such as 48.0 ± 11.2 ($r \approx 2000$), 63.3 ± 9.0 ($r \approx 660$), 103.5 ± 15.8 ($r \approx 200$), 151.6 ± 16.6 ($r \approx 10$), and 198.4 ± 18.5 ($r \approx 1$) nm have been obtained. The formation process of the different spherical sizes involved a gradual color change of the gold nanoparticles from red to purple or blue, as evidenced by the spectral evolution of the surface plasmon (SP) resonance band (Figure 2). In comparison with the SP band at 520 nm observed for **1**/**Au**, the extent of this red shift is inversely related to the concentration of **2**. The SP band wavelength showed a shift from 580 to 780 nm as a result of the decrease of $r$. In the case of a ratio of ∼2000, there is an excess of **2** to make a full monolayer encapsulation on the 5.1-nm sized nanoparticle core, in comparison to the estimate from a model calculation (200−300 molecules of **2** per nanoparticle). Conversely, the lower concentration corresponds to $r \approx 1$ (ca. one molecule of **2** per nanoparticle). The spectral envelope of the SP band apparently consists of two overlapping bands. At the lower concentration of **2**, these two bands are clearly resolved at 520 and 780 nm, and an isosbestic point is displayed at 560 nm indicative of the involvement of two major species in the reaction solution (see Supporting Information). The final product at low concentrations of **2** eventually precipitated after 1−2 days, but remained soluble for many weeks when $r \approx 2000$ was used.

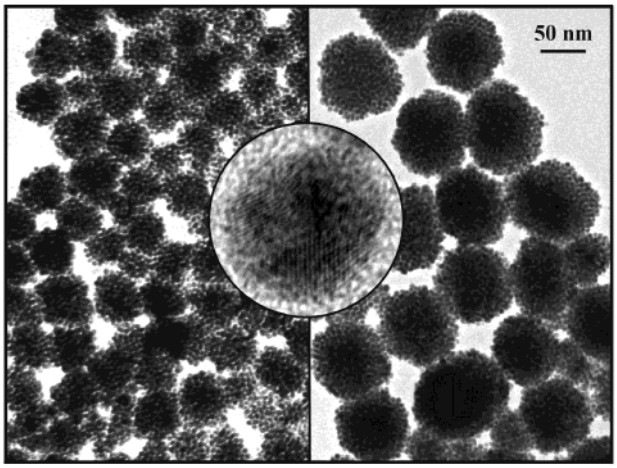


***Figure 1.*** TEM micrographs showing the spherical assemblies obtained from two different [**2**]:[**1**/**Au**] ratios: (a, left) $r \approx 660$ ([**1**/**Au**] = 0.1 $\mu$M, [**2**] = 66 $\mu$M). (b, right) $r \approx 200$ ([**1**/**Au**] = 0.1 $\mu$M, [**2**] = 20 $\mu$M). Both images have the same scale bar. Insert: HRTEM of an individual **1**/**Au** nanoparticle.

The range of sizes (30−200 nm) of spherical assemblies that can be produced simply by varying the concentration of **2** is

[†] State University of New York at Binghamton.
[‡] The University of North Carolina at Charlotte.
[§] Brookhaven National Laboratory.


**10.1021/ja0363866 CCC: $25.00** 

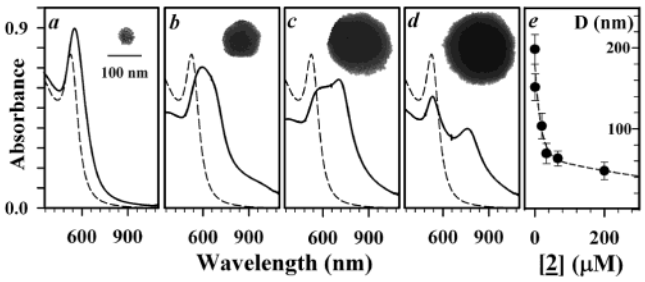


***Figure 2.*** SP band for **1**/**Au** in toluene (0.1 $\mu$M, dashed line) and the final spectra upon addition of **2** (200 (a), 20 (b), 0.8 (c), and 0.08 $\mu$M (d); $r \approx$ 2000 (a), 200 (b), 10 (c), and 1 (d)). TEM micrographs of individual spheres for the corresponding samples are included as inserts (all have the same scale bar). A plot of the spherical diameter (D) vs [**2**] is included (d), which can be fitted by $y = ae^{-bx} + ce^{-dx}$ ($a = 1.13 \times 10^2$, $b = 6.0 \times 10^{-2}$, $c = 6.59 \times 10$, $d = 1.60 \times 10^{-3}$).

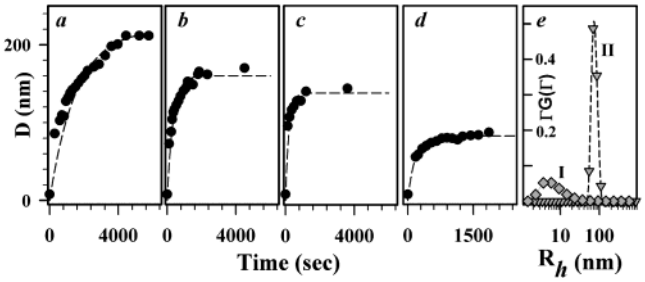


***Figure 3.*** (a−d) DLS data for the evolution of spherical size as a function of time for a series of **2** concentrations: ([**1**/**Au**] = 0.0072 $\mu$M, and [**2**] = 0.16 (a), 0.32 (b), 1.25 (c), 25.0 $\mu$M (d)). The data are fitted with $d = d_0[1 - \exp[-(kt)^n]$. (e) A plot of $\Gamma G(\Gamma)$ versus $R_h$ from CONTIN analysis for the isolated (I) and the assembled **1**/**Au** (II).

remarkable. A plot of the average diameter of the spheres versus concentration of **2** (Figure 2e) shows that the size increases exponentially with decreasing concentration.

Dynamic light scattering (DLS) measurements performed in situ provided further evidence for the controlled growth of spherical assemblies in solution. The diameter of the spherical assembly is plotted against the reaction time at four different concentrations of **2** (Figure 3). The size was determined from the hydrodynamic radii of the assemblies based on CONTIN analysis of the characteristic line width ($\Gamma$).[20,21] There are three important findings in these data sets. First, the increase of spherical diameter ($D$) with time can be fitted to a modified theoretical model of crystallization and growth[22] where the critical growth exponent is close to 1, which is indicative of lower growth dimensionality, consistent with the spherical shape. The rate constant increases with concentration of the mediator (Figure 3a−d). Second, the final size of the nanoparticle assemblies increases with decreasing concentration of ligand, which is consistent with UV−vis and TEM data. The reversal of these assemblies upon addition of a thiol (e.g., decanethiol) to the reaction solution was also observed (Supporting Information). Finally, the spherical assemblies are highly monodispersed, as evidenced by the sharpness of the peak in a plot of $\Gamma G(\Gamma)$ versus $R_h$ (e.g., Figure 3e). These findings provided further evidence supporting the **2**-based mediation mechanism for the size controllability. We note that DLS was previously utilized to monitor the assembly of gold nanoparticles in the presence of DNA.[23] Our DLS data thus demonstrate for the first time size-controllability of nanoparticle assembly processes.

The number of thioether groups in **2** was also found to impact the assembly of nanoparticles, including their size and subtle differences in reaction kinetics. There was no indication of any assembly process when a bidentate ligand was used. The use of bulkier thioethers $Me_{4-n}Si(CH_2SBu^t)_n$ ($n = 3$ and 4) did not produce any significant assembly either.

In conclusion, we have demonstrated for the first time the ability to control the size of nanoparticle assemblies via a novel mediation-template strategy. A combination of the ligand mediation, the surfactant templating,[18] and their relative concentrations served as the driving forces to determine the spherical formation in controllable sizes. We are currently correlating these control factors and manipulating the structures of **1** and **2** in terms of chain length and number of ligands for the control of both size and shape (e.g., rods, cubes, etc.) of the nanoparticle assemblies.

**Acknowledgment.** Financial support of this work from the ACS-PRF and 3M Corp. is gratefully acknowledged. M.M.M. thanks the U.S. DoD (ARO) for support via a National Defense Science & Engineering Graduate Fellowship. D.R. also thanks Research Corp. for a Cottrell College Science Award, and T.L. acknowledges support from the U.S. DOE, Division of Materials Science (DE-AC02-98CH10886).

**Supporting Information Available:** Additional data (UV−vis and DLS) (PDF). This material is available free of charge via the Internet at http://pubs.acs.org.

## References

(1) Brust, M.; Walker, M.; Bethell, D.; Schiffrin, D. J.; Whyman, R. *J. Chem. Soc., Chem. Commun.* **1994**, 801.
(2) Templeton, A. C.; Wuelfing, W. P.; Murray, R. W. *Acc. Chem. Res.* **2000**, *33*, 27.
(3) Andres, R. P.; Bielefeld, J. D.; Henderson, J. I.; Janes, D. B.; Kolagunta, V. R.; Kubiak, C. P.; Mahoney, W. J.; Osifchin, R. G. *Science* **1996**, *273*, 1690.
(4) Freeman, R. G.; Grabar, K. C.; Allison, K. J.; Bright, R. M.; Davis, J. A.; Guthrie, A. P.; Hommer, M. B.; Jackson, M. A.; Smith, P. C.; Walter, D. G.; Natan, M. J. *Science* **1995**, *267*, 1629.
(5) Zamborini, F. P.; Hicks, J. F.; Murray, R. W. *J. Am. Chem. Soc.* **2000**, *122*, 4514.
(6) Elghanian, R.; Storhoff, J. J.; Mucic, R. C.; Letsinger, R. L.; Mirkin, C. A. *Science* **1997**, *277*, 1078.
(7) Mirkin, C. A.; Letsinger, R. L.; Mucic, R. C.; Storhoff, J. J. *Nature* **1996**, *382*, 607.
(8) Alivisatos, A. P.; Johnsson, K. P.; Peng, X. G.; Wilson T. E.; Loweth, C. J.; Bruchez, M. P.; Schultz, P. G. *Nature* **1996**, *382*, 609.
(9) Mbindyo, J. K. N.; Reiss, B. D.; Martin, B. R.; Keating, C. D.; Natan, M. J.; Mallouk, T. E. *Adv. Mater.* **2001**, *13*, 249.
(10) Zheng, W. X.; Maye, M. M.; Leibowitz, F. L.; Zhong, C. J. *Anal. Chem.* **2000**, *72*, 2190.
(11) Boal, A. K.; Rotello, V. M. *J. Am. Chem. Soc.* **2002**, *124*, 5019.
(12) Shon, Y. S.; Mazzitelli, C.; Murray, R. W. *Langmuir* **2001**, *17*, 7735.
(13) Li, X. M.; de Jong, M. R.; Inoue, K.; Shinkai, S.; Huskens, J.; Reinhoudt, D. N. *J. Mater. Chem.* **2001**, *11*, 1919.
(14) Boal, A. K.; Ilhan, F.; DeRouchey, J. E.; Thurn-Albrecht, T.; Russell, T. P.; Rotello, V. M. *Nature* **2000**, *404*, 746.
(15) Brousseau, L. C.; Novak, J. P.; Marinakos, S. M.; Feldheim, D. L. *Adv. Mater.* **1999**, *11*, 447.
(16) Maye, M. M.; Chun, S. C.; Han, L.; Rabinovich, D.; Zhong, C. J. *J. Am. Chem. Soc.* **2002**, *124*, 4958.
(17) Yim, H. W.; Tran, L. M.; Dobbin, E. D.; Rabinovich, D.; Liable-Sands, L. M.; Incarvito, C. D.; Lam, K.-C.; Rheingold, A. L. *Inorg. Chem.* **1999**, *38*, 2211.
(18) Israelachvilli, J. N.; Mitchell, D. J.; Ninham, B. W. *J. Chem. Soc., Faraday Trans. 2* **1976**, *72*, 1525.
(19) Fink, J.; Kiely, C. J.; Bethell, D.; Schiffrin, D. *J. Chem. Mater.* **1998**, *10*, 922.
(20) Liu, T. *J. Am. Chem. Soc.* **2003**, *125*, 312.
(21) DLS measures the intensity-time correlation function $G(2)(\Gamma)$ by means of a BI-9000 AT multichannel digital correlator: $G(2)(\Gamma) = A(1+b|g(1)(\tau)|2)$. Details are provided in the Supporting Information.
(22) Han, L.; Maye, M. M.; Leibowitz, F. L.; Ly, N. K.; Zhong, C. J. *J. Mater. Chem.* **2001**, *11*, 1259.
(23) Storhoff, J. J.; Lazarides, A. A.; Mucic, R. C.; Mirkin, C. A.; Letsinger, R. L.; Schatz, G. C. *J. Am. Chem. Soc.* **2000**, *122*, 4640.

JA0363866